Formation of Al Nanostructures on Alq3: An in Situ Grazing Incidence Small Angle X-ray Scattering Study during Radio Frequency Sputter Deposition

ARTICLE *in* JOURNAL OF PHYSICAL CHEMISTRY LETTERS · SEPTEMBER 2013

Impact Factor: 7.46 · DOI: 10.1021/jz401585d

14 AUTHORS, INCLUDING:

Shun Yu
KTH Royal Institute of Technology
40 PUBLICATIONS **319** CITATIONS
SEE PROFILE

Ralph Döhrmann
Deutsches Elektronen-Synchrotron
42 PUBLICATIONS **661** CITATIONS
SEE PROFILE

Matthias Schwartzkopf
Deutsches Elektronen-Synchrotron
19 PUBLICATIONS **244** CITATIONS
SEE PROFILE

Stephan V Roth
Deutsches Elektronen-Synchrotron
364 PUBLICATIONS **3,272** CITATIONS
SEE PROFILE

THE JOURNAL OF PHYSICAL CHEMISTRY Letters

Letter

pubs.acs.org/JPCL

Formation of Al Nanostructures on Alq3: An in Situ Grazing Incidence Small Angle X-ray Scattering Study during Radio Frequency Sputter Deposition

Shun Yu,*[,†] Gonzalo Santoro,[†] Kuhu Sarkar,[‡] Benjamin Dicke,[†] Philipp Wessels,[§] Sebastian Bommel,[†,∥] Ralph Döhrmann,[†] Jan Perlich,[†] Marion Kuhlmann,[†] Ezzeldin Metwalli,[‡] Johannes F. H. Risch,[†] Matthias Schwartzkopf,[†] Markus Drescher,[§] Peter Müller-Buschbaum,[‡] and Stephan V. Roth*[,†]

[†]Deutsches Elektronen-Synchrotron (DESY), Notkestraße 85, D-22607 Hamburg, Germany

[‡]Lehrstuhl für Funktionelle Materialien, Physik-Department, Technische Universität München, James-Franck-Straße 1, D-85748 Garching, Germany

[§]Institut für Experimentalphysik, Universität Hamburg, Luruper Chaussee 149, D-22761 Hamburg, Germany

[∥]Institut für Physik, Humboldt-Universität zu Berlin, Newtonstraße 15, D-12489 Berlin, Germany

Supporting Information

ABSTRACT: The formation of metal/organic interfaces is a complicated process involving chemical interaction, physical nucleation and diffusion, and thin film growth. It is closely related to the performance of organic electronic devices. To understand this process, we investigate the system of aluminum (Al) and tris(8-hydroxyquinolinato)-aluminum (Alq3) as a model, owing to the well-known strong chemical interaction between both and their close technological relevance to organic light emitting devices. By using grazing small angle incidence X-ray scattering (GISAXS), we follow the Al thin film development on top of Alq3 during radio frequency (rf) sputter deposition in real-time and without interrupting the growth process. Three growth stages have been clearly distinguished: Al diffusion into Alq3, Al/Alq3 complex agglomeration and self-assembled Al pillar nanostructure thin film development. Thus in situ GISAXS yields the fundamental insights into the formation of the metal/organic interface for small organic semiconductor devices, prepared via vacuum based deposition techniques.

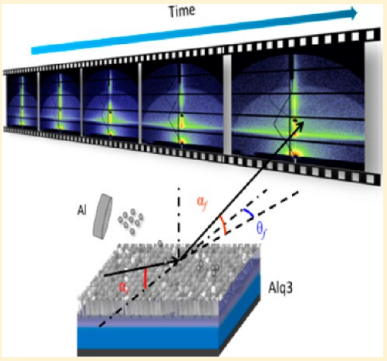

SECTION: Physical Processes in Nanomaterials and Nanostructures

The advancing of organic electronics demands a deep understanding of the interface structure and properties between metal thin films and organic layers.[1,2] In general, depending on the order of the deposition—organic-on-metal (organic/metal) and metal-on-organic (metal/organic)—two types of interfaces can be formed with distinctive structures and properties. For the organic/metal interface, usually a sharp interface is found, whereas for metal/organic interfaces, a gradient metal diffusion layer within the molecular thin film can be present. Depending on the atomic or molecular interaction, different charge transfer mechanisms can be generated.[3,4] The thickness of the diffusion layer is depending on the applied metal deposition techniques.[5−8] Upon diffusing into the organic layer, the metal atoms will modify the properties of the organic film and this interaction will also tune the growth mode of the metal thin film on top.

In applications, a typical organic electronic device, such as organic light emitting diodes (OLEDs), consists of a multilayer structure, incorporating different organic semiconductors and metallic materials as electrode contacts.[9] Since the first OLED device was fabricated by Tang et al., tris(8-hydroxyquinolinato)aluminum (Alq3) has been one of the key materials in the research focus.[10] The interaction between metal electrodes (most commonly used are Mg, Al, Ag, and Au) and Alq3 at a molecular level has been intensively studied by different spectroscopy techniques[6−8,11−13] and theoretical studies.[14−16] All results confirm that reactive metals, such as Mg and Al, will form a compound with Alq3 via the oxygen atoms in the molecule, while noble metals, e.g., Ag and Au, are less reactive with Alq3. Recently, Fladischer et al. have shown that the combination of X-ray reflectivity (XRR) and transmission electron microscopy (TEM) can provide detailed information of the device structure: Depending on the deposition method and deposition parameters, Ag can selectively diffuse into the Alq3 thin film.[5]

Sputtering is a typical thin film deposition technique. Although the plasma and the high kinetic energy atoms may cause damage to an organic film, Suzuki et al. have reported successful deposition of Al, Mg, and Mg:Ag on top of Alq3 by radio frequency (rf) sputter deposition, not only *without*

Received: July 25, 2013
Accepted: September 5, 2013
Published: September 5, 2013

dx.doi.org/10.1021/jz401585d | J. Phys. Chem. Lett. 2013, 4, 3170−3175

damaging its chemical structure but also with improved thin film characteristics.[17,18] From the application point of view, researchers often add a buffer layer between Alq3 and the metal to prevent the metal diffusion for a better device performance.[19] However, a fundamental question remains unsolved for the metal/organic interface: What is the relationship between the metal film structure and the strong chemical interaction?

Considering that growth of a metal layer is a dynamic process, the ability to follow in real-time the thin film growth in a nondestructive and noninterrupting fashion becomes highly desirable. The progresses of grazing incidence small-angle X-ray scattering (GISAXS)[20−24] has made it an ideal tool for the investigation of nanostructures assembly and evolution[25−28] and in situ characterization during vacuum based thin film fabrications.[29−32] In this work, we exploit in situ GISAXS to investigate the initial thin film development of Al on top of Alq3 in real-time, given the well-known chemical interaction between both. The structure evolution is recorded continuously in reciprocal space, without interrupting the sputtering process.[33,34] Thus it provides first-hand information on how the structure evolves from deposition atom to the nanostructured thin film. (experimental details: see the Supporting Information)

The selected two-dimensional (2D) GISAXS data before and during sputter deposition show the evolution of lateral structures on the surface, along the horizontal direction (q_y) in the Yoneda region, Figure 1a−d. In the vertical direction (q_z), the sputtered Al layer introduces an additional modulation of the intensity. These changes in the scattering patterns are related to the structural changes in the film which are easily demonstrated from the horizontal and vertical profiles versus deposited film thickness (Figure 1e and 1f). For the first 3.0 nm Al deposition, the intensity in the vertical cuts gets clearly enhanced, as shown in Figure 1f, while no intensity increases along the horizontal direction, as seen in Figure 1e. We identify this as the first growth stage (Stage I). In the following Stage II, a sharp structure transition occurs parallel to the sample surface shown in the horizontal profile with the feature initially centered around q_y = 0.50 nm^{-1}. Accordingly, a modulation along the q_z direction also enters the detection region and shifts toward lower q_z. In the subsequent deposition, the horizontal profile feature slowly shifts to smaller q_y values, indicating a formation of larger structures. After 10.0 nm Al deposition, a new lateral structure abruptly develops (Figure 1e). It is clearly distinguished from the one developed in Stage II and appears with the maximum intensity at higher q_y values, suggesting the formation of yet smaller structures on top of the deposited film. This period is named Stage III. Different from this abrupt intensity change along q_y, the intensity modulation along q_z develops rather continuously as the Al thickness increases in both Stage II and III.

Detailed structural developments in both horizontal and vertical profiles are revealed by plotting line cuts from selected Al thicknesses in Figure 2a,b. During sputter deposition the Al film thickness increases (from bottom to top) causing marked changes in the intensity. In Figure 2a, a clear shoulder can be found at q_y = 0.06 nm^{-1} (marked by dashed line), which exists before the deposition and does not shift during the sputtering process. Thus it can be unambiguously assigned to large Alq3 structures with a lateral size of about 100 nm. This component shows no obvious intensity variation during the sputter deposition so that we can exclude the preferential Al adsorption and agglomeration at these structures.[35] At larger q_y values, a

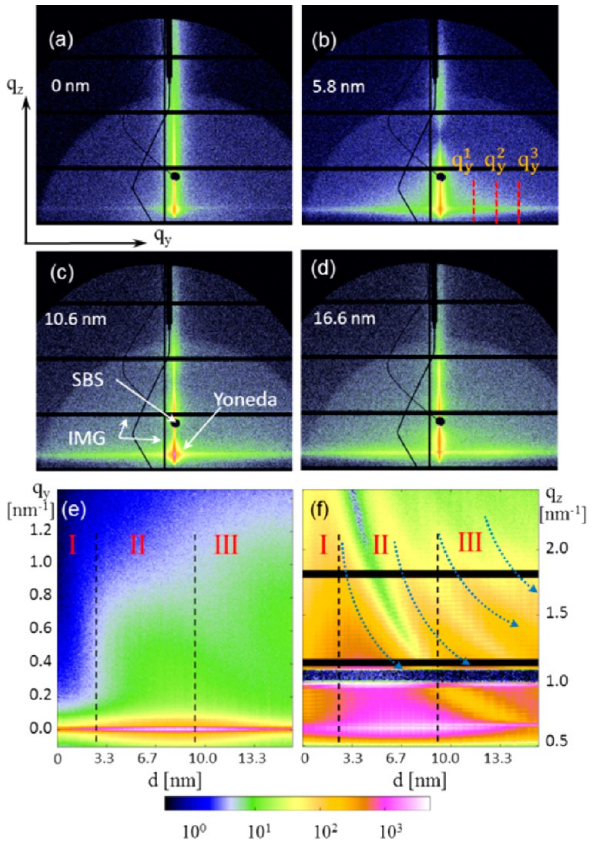

Figure 1. Two-dimensional (2D) GISAXS patterns of Al sputtered on top of Alq3 thin film at 0 nm (a), 5.8 nm (b), 10.6 nm (c), and 16.6 nm (d). In (a), black solid lines indicate q_y and q_z coordination; three red dot lines q_y^1, q_y^2 and q_y^3 mark the position for off-center vertical cuts in (b); specular beam stop (SBS) detector, intermodular gap (IMG) and Yoneda region are marked in (c); q_y and q_z line cuts versus sputtered thickness are plotted in (e) and (f), respectively and are divided into three growth stages (I, II and III) via black dashed lines, according to the intensity change of the horizontal profile. The blue dot arrows in (f) illustrate the development of q_z modulations induced by Al deposition. The intensity of (e) and (f) is indicated by the color scale at the bottom.

side peak appears during increasing the sputtered film thickness. Red and blue color highlights the side peak at Stage II and III, respectively. The peak position is fitted with a single Lorentzian function (inset in Figure 2a). It shifts from larger to smaller q_y values in Stage II. The transition from Stage II to III occurs between an Al thickness of 10.0 and 12.0 nm, where this trend in the peak movement is reversed. In Stage III the peak shifts toward higher q_y values until it becomes dominant at 0.70 nm^{-1} after deposition of 12.0 nm Al. Figure 2b shows vertical cuts with the q_z range being zoomed-in the region between 0.50 and 0.98 nm^{-1}. A modulation in the intensity is clearly resolved along the q_z (Figure S1 in Supporting Information). This is an indication that the Alq3 thin film shows a good surface roughness correlation with the silicon substrate; During Al deposition, the roughness correlation remains. An interesting feature of the scattering profiles along q_z, is the intensity shifts from lower to higher q_z values (between 0.60 and 0.70 nm^{-1} in Figure 1f). This regions is located at the so-called Yoneda peak,[36] which appears at the position of the material specific critical angle (α_c). It is a function of the real part of X-ray refractive index (δ) by $\alpha_c = (2\delta)^{1/2}$, where δ is proportional to the average charge density of

dx.doi.org/10.1021/jz401585d | J. Phys. Chem. Lett. 2013, 4, 3170−3175

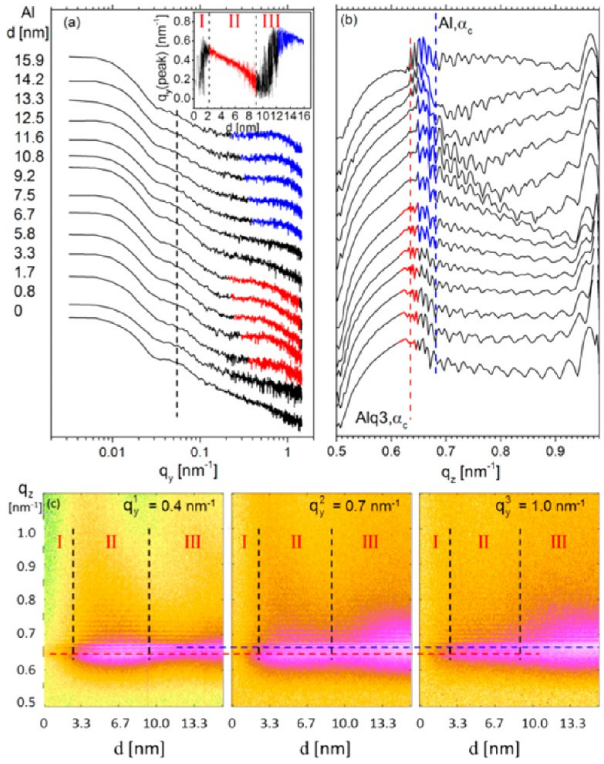

Figure 2. (a) Horizontal cuts from the 2D GISAXS data for selected thicknesses (shifted along the intensity axis); the vertical dashed line marks the large features in the Alq3 thin film, which remains constant during the entire sputtering. Inset shows the fitted peak position of the Al related structure versus sputtered thickness using a single Lorentzian component which is divided into three stages, accordingly. In (a), red and blue colors mark the lateral features corresponding to Stage II and III. (b) Vertical cuts from the 2D GISAXS data for selected thicknesses (shifted along the intensity axis); red and blue highlighted areas represent the dominant intensity in the Yoneda region during the deposition; the theoretical critical angle for Al and Alq3 are marked as vertical blue and red dashed lines, respectively. (c) Off-center cut at q_y^1 = 0.40 nm^{-1} (left), q_y^2 = 0.70 nm^{-1} (middle) and q_y^3 = 1.00 nm^{-1} (right) versus film thickness. Stage I, II and III are indicated. Horizontal red and blue dashed lines mark the different Yoneda positions corresponding to the highlighted q_z value in (b).

the material. Thus, this peak position indicates chemical sensitivity. The observed upward shift reflects the increase of elemental average charge density at the interface due to Al deposition. At 13 keV, the theoretical α_c of Al and Alq3 (density:[37] 1.3 g/mm^3) are 0.14° and 0.10°, respectively. The corresponding q_z values are at 0.68 nm^{-1} and 0.63 nm^{-1} at the used incidence angle of 0.45° (indicated by blue and red vertical line in Figure 2b). We use red and blue colors to highlight the dominant features at the Yoneda region. For Stages I and II, the highest intensity (in red) develops from 0.63 to 0.65 nm^{-1}, which is close to the Alq3 theoretical value, indicating that Al diffuses into Alq3 and thereby increases the average charge density by forming Al/Alq3 complexes.[14,16] The successive sputtering in Stage III leads to the dominant feature rapidly developing between 0.65 and 0.68 nm^{-1} (in blue) and approaching the theoretical α_c value of Al. It implies the formation of a pure Al structure. However, the theoretical value of bulk Al is not reached, which suggests that a lower density structure should form on the surface.

In Figure 2(c), three off-center vertical cuts at 0.40 nm^{-1} (q_y^1), 0.70 nm^{-1} (q_y^2) and 1.00 nm^{-1} (q_y^3) versus film thickness are shown. The off-center maxima are highlighted by the horizontal red and blue dashed lines in the three panels of Figure 2c at the positions of 0.64 nm^{-1} and 0.67 nm^{-1}, i.e., close to the theoretical critical angles of Alq3 and Al, respectively. When the sputter deposition starts, in Stage I the off-center vertical cuts show an average intensity increase, indicating the stronger scattering due to Al incorporation. In Stage II, the dominant intensity of the off-center cuts is aligned with the Al/Alq3 Yoneda peak, meaning these lateral structures originate from Al/Alq3 complexes; in Stage III, the maximum intensity in the off-center cuts is aligned with the Al Yoneda peak position, indicating that the lateral structures at this stage are mainly Al related.

FESEM images are shown in Figure 3. An overview image of the sputtered surface is presented in Figure 3a. Some large

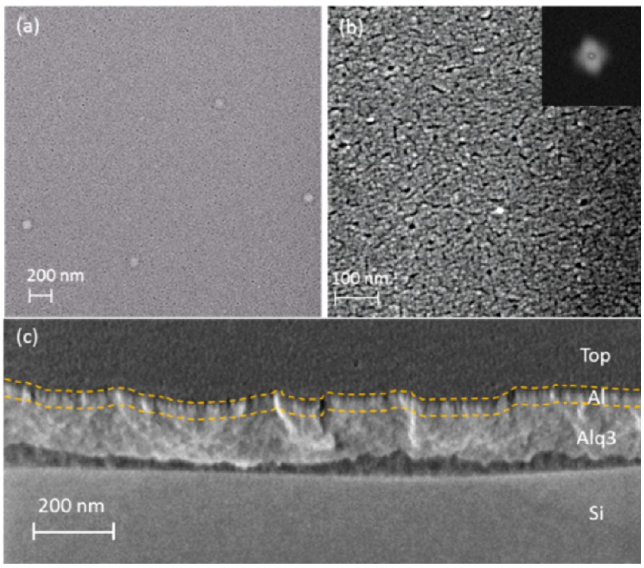

Figure 3. Field emission scanning electron microscopy (FESEM) images of Al sputtered on top of Alq3: overview (a) and detailed structure (b); inset in (b) is the corresponding Fast Fourier Transformation (FFT). Cross section FESEM image of Al/Alq3/Si structure (c); the double yellow dashed lines highlight the cross section of Al layer, which shows pillar like structure.

clusters around 100 nm diameters are seen, which might be related to the Alq3-feature at q_y 0.06 nm^{-1} in Figure 2a. Besides these features, the surface shows a good homogeneity. A magnified image of the flat area is shown in Figure 3b. A porous structure is visible at higher magnification. This also supports our interpretation based on the Al Yoneda peak position, confirming the fact that sputtered Al layer shows lower average charge density compared to the bulk material. The Fast Fourier Transformation (FFT) shows an orthogonal distribution with the center value corresponding to ~10 nm in real space. The intensities of the two perpendicular lobes are not the identical. This result suggests that these structures are preferentially oriented along the orientation of the two lobes. By cleaving and tilting the specimen up to 60°, the cross section was probed (Figure 3c). Above the silicon substrate, the Alq3 layer shows a rather homogeneous structure, while the Al layer (highlighted by the dashed lines) displays a clear pillar-like structure. This readily sheds light on the particle shape needed for the GISAXS simulation.

dx.doi.org/10.1021/jz401585d | J. Phys. Chem. Lett. 2013, 4, 3170−3175

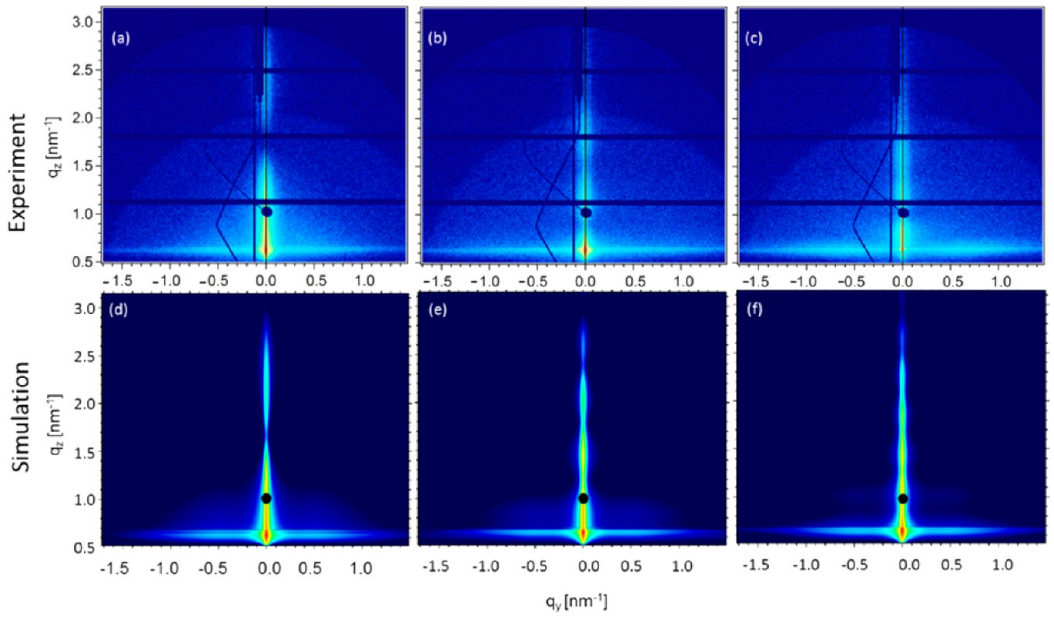

Figure 4. (a–c) Experimental 2D GISAXS data at 5.3 nm, 10.6 and 16.6 nm Al thickness; (d–f) corresponding simulation with Black dots marking the SBS.

Thus we assume a 2D square paracrystal distribution of a lattice constant around 10 nm for the Al nanostructures in the simulation of the GISAXS patterns. The results of these simulations are shown in Figure 4d–f and compared with the corresponding experimental data (Figure 4a–c). We used a truncated pyramid particle shape with the bottom width of 3 and 4 nm and a very steep slope of 85°. A cylinder structure can be excluded due to strong lateral scattering at large q_z values. Although the Al oxide layer might modify the Al structure observed by FESEM, our simulation based on the 2D paracrystal (extracted from the FFT analysis) reproduced the experimental data reasonably well for the 2D intensity distribution.

Combining all the information, we summarize the growth process in Scheme 1. We suggest that in Stage I, Al diffuses into the Alq3 thin film and forms Al/Alq3 complexes via Al–O bond. At this point, the chemical interaction at atomic level changes the average charge density at the thin film surface, which renders the vertical cut intensity change shown in Figure 1f. In Stage II Al/Alq3 complexes start to agglomerate due to the interaction between the successively deposited Al and the Al/Alq3 complexes formed in Stage I, which has been proposed by theoretical studies as well.[16] In Stage III, further deposited Al starts to grow as pillar-like nanostructured adlayer on top. This three-stage growth of Al on Alq3 is different from perfect layer-by-layer growth of Al sputtered on top of P3HT reported by Kaune et al.,[30] where no side peaks along q_y direction can be found during the entire sputter process. Moreover, it can also be distinguished from the case of gold sputtered on polymer[21,29] and silicon,[31] where hemispherical and/or spherical shaped nanocluster models are used to describe the dynamic growth with a single peak shifting from the large q_y (≥4 nm^{-1}) toward lower q_y values during sputtering.

Scheme 1. The Schematics of Three Stages Growth Mode of Al Sputtered on Alq3

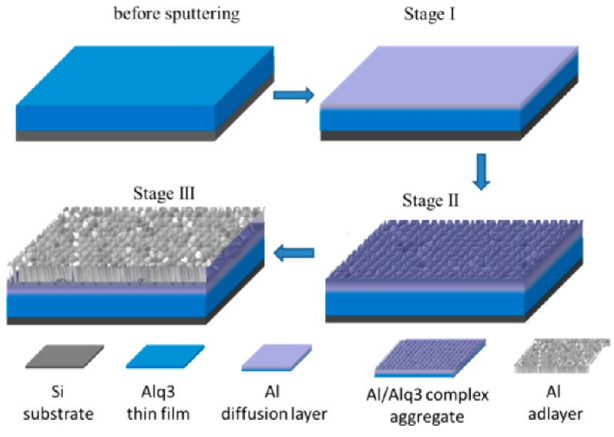

In this study, we have successfully identified a three-stage nanostructure thin film formation on top of Alq3. The investigation of the intensity changes along the Yoneda wing correlate Al/Alq3 and Al lateral structures to the chemical component within the thin film. The self-assembled nanostructures are also supported by FESEM images and simulations of the GISAXS data. The outcome of this work is helpful to clarify the complex metal thin films structure evolution on small molecular films. Therefore it is meaningful for general understanding of the metal/organic interfacial structure prepared via vacuum-based deposition.

■ ASSOCIATED CONTENT

Supporting Information

Detailed experimental information; overview of q_z profile; magnified Yoneda profile; ex situ XRR measured on sample. This material is available free of charge via the Internet at http://pubs.acs.org.

■ AUTHOR INFORMATION

Corresponding Authors

*E-mail: shun.yu@desy.de.
*E-mail: stephan.roth@desy.de.

dx.doi.org/10.1021/jz401585d | J. Phys. Chem. Lett. 2013, 4, 3170–3175

Notes

The authors declare no competing financial interest.

■ ACKNOWLEDGMENTS

S.Y. acknowledges the Knut och Alice Wallenberg foundation for the kind financial support. P.M.-B., E.M., and K.S. acknowledge financial support by TUM.solar in the frame of the Bavarian Collaborative Research Project "Solar technologies go Hybrid" (SolTec) and by the GreenTech Initiative (Interface Science for Photovoltaics - ISPV) of the EuroTech Universities. Portions of this research were carried out at the light source PETRA III at DESY, a member of the Helmholtz Association (HGF). Dr. David Babonneau is acknowledged for helpful discussion, and Erik Braden for the XRR measurements.

■ REFERENCES

(1) Popok, V. N.; Barke, I.; Campbell, E. E. B.; Meiwes-Broer, K.-H. Cluster−Surface Interaction: from Soft Landing to Implantation. *Surf. Sci. Rep.* **2011**, *66*, 347−377.
(2) Bittner, A. M. Clusters on Soft Matter Surfaces. *Surf. Sci. Rep.* **2006**, *61*, 383−428.
(3) Braun, S.; Salaneck, W. R.; Fahlman, M. Energy-Level Alignment at Organic/Metal and Organic/Organic Interfaces. *Adv. Mater.* **2009**, *21*, 1450−1472.
(4) Vázquez, H.; Dappe, Y. J.; Ortega, J.; Flores, F. Energy Level Alignment at Metal/Organic Semiconductor Interfaces: "Pillow" Effect, Induced Density of Interface States, and Charge Neutrality Level. *J. Chem. Phys.* **2007**, *126*, 144703−144710.
(5) Fladischer, S.; Neuhold, A.; Kraker, E.; Haber, T.; Lamprecht, B.; Salzmann, I.; Resel, R.; Grogger, W. Diffusion of Ag Into Organic Semiconducting Materials: A Combined Analytical Study Using Transmission Electron Microscopy and X-ray Reflectivity. *ACS Appl. Mater. Interfaces* **2012**, *4*, 5608−5612.
(6) Turak, A.; Grozea, D.; Feng, X. D.; Lu, Z. H.; Aziz, H.; Hor, A. M. Metal/AlQ3 Interface Structures. *Appl. Phys. Lett.* **2002**, *81*, 766−768.
(7) Shen, C.; Kahn, A. The Role of Interface States in Controlling the Electronic Structure of AlQ3/Reactive Metal Contacts. *Org. Electr.* **2001**, *2*, 89−95.
(8) Shen, C.; Kahn, A.; Schwartz, J. Chemical and Electrical Properties of Interfaces between Magnesium and Aluminum and Tris-(8-Hydroxy Quinoline) Aluminum. *J. Appl. Phys.* **2001**, *89*, 449−459.
(9) Gather, M. C.; Köhnen, A.; Meerholz, K. White Organic Light-Emitting Diodes. *Adv. Mater.* **2011**, *23*, 233−248.
(10) Tang, C. W.; VanSlyke, S. A. Organic Electroluminescent Diodes. *Appl. Phys. Lett.* **1987**, *51*, 913−915.
(11) Miyamae, T.; Ito, E.; Noguchi, Y.; Ishii, H. Characterization of the Interactions between Alq 3 Thin Films and Al Probed by Two-Color Sum-Frequency Generation Spectroscopy. *J. Phys. Chem. C* **2011**, *115*, 9551−9560.
(12) Rajagopal, A.; Kahn, A. Photoemission Spectroscopy Investigation of Magnesium−Alq3 Interfaces. *J. Appl. Phys.* **1998**, *84*, 355−358.
(13) Nguyen, T. P.; Ip, J.; Jolinat, P.; Destruel, P. XPS and Sputtering Study of the Alq3/Electrode Interfaces in Organic Light Emitting Diodes. *Appl. Surf. Sci.* **2001**, *172*, 75−83.
(14) Yanagisawa, S.; Lee, K.; Morikawa, Y. First-principles Theoretical Study of Alq3Al Interfaces: Origin of the Interfacial Dipole. *J. Chem. Phys.* **2008**, *128*, 244704−2447015.
(15) Curioni, A.; Andreoni, W. Metal−Alq 3 Complexes: The Nature of the Chemical Bonding. *J. Am. Chem. Soc.* **1999**, *121*, 8216−8220.
(16) Takeuchi, K.; Yanagisawa, S.; Morikawa, Y. First-Principles Molecular Dynamics Study of Al/Alq3 Interfaces. *Sci. Technol. Adv. Mater.* **2007**, *8*, 191−195.
(17) Suzuki, H.; Hikita, M. Organic Light-Emitting Diodes with Radio Frequency Sputter-Deposited Electron Injecting Electrodes. *Appl. Phys. Lett.* **1996**, *68*, 2276−2278.
(18) Suzuki, H. Fabrication of Electron Injecting Mg:Ag Alloy Electrodes for Organic Light-Emitting Diodes with Radio Frequency Magnetron Sputter Deposition. *Appl. Phys. Lett.* **1996**, *69*, 1611−1613.
(19) Kim, H.-K.; Kim, S.-W.; Lee, K.-S.; Kim, K. H. Direct Al Cathode Layer Sputtering on LiF/Alq3 Using Facing Target Sputtering with a Mixture of Ar and Kr. *Appl. Phys. Lett.* **2006**, *88*, 083513−083515.
(20) Renaud, G.; Lazzari, R.; Leroy, F. Probing Surface and Interface Morphology with Grazing Incidence Small Angle X-ray Scattering. *Surf. Sci. Rep.* **2009**, *64*, 255−380.
(21) Roth, S. V.; Walter, H.; Burghammer, M.; Riekel, C.; Lengeler, B.; Schroer, C.; Kuhlmann, M.; Walther, T.; Sehrbrock, A.; Domnick, R.; et al. Combinatorial Investigation of the Isolated Nanoparticle to Coalescent Layer Transition in a Gradient Sputtered Gold Nanoparticle Layer on Top of Polystyrene. *Appl. Phys. Lett.* **2006**, *88*, 021910−021912.
(22) Roth, S. V.; Burghammer, M.; Riekel, C.; Müller-Buschbaum, P.; Diethert, A.; Panagiotou, P.; Walter, H. Self-Assembled Gradient Nanoparticle-Polymer Multilayers Investigated by an Advanced Characterization Method: Microbeam Grazing Incidence X-ray Scattering. *Appl. Phys. Lett.* **2003**, *82*, 1935−1937.
(23) Müller-Buschbaum, P. Grazing Incidence Small-Angle X-ray Scattering: An Advanced Scattering Technique for the Investigation of Nanostructured Polymer Films. *Anal. Bioanal. Chem.* **2003**, *376*, 3−10.
(24) Müller-Buschbaum, P.; Roth, S. V; Burghammer, M.; Diethert, A.; Panagiotou, P.; Riekel, C. Multiple-Scaled Polymer Surfaces Investigated with Micro-Focus Grazing-Incidence Small-Angle X-ray Scattering. *Europhys. Lett.* **2003**, *61*, 639−645.
(25) Ruderer, M. A.; Meier, R.; Porcar, L.; Cubitt, R.; Müller-Buschbaum, P. Phase Separation and Molecular Intermixing in Polymer−Fullerene Bulk Heterojunction Thin Films. *J. Phys. Chem. Lett.* **2012**, *3*, 683−688.
(26) Kim, H. J.; Kim, J. W.; Lee, H. H.; Kim, T.-M.; Jang, J.; Kim, J.-J. Grazing Incidence Small-Angle X-ray Scattering Analysis of Initial Growth of Planar Organic Molecules Affected by Substrate Surface Energy. *J. Phys. Chem. Lett.* **2011**, *2*, 1710−1714.
(27) Chaâbane, N.; Lazzari, R.; Jupille, J.; Renaud, G.; Avellar Soares, E. CO-Induced Scavenging of Supported Pt Nanoclusters: A GISAXS Study. *J. Phys. Chem. C* **2012**, *116*, 23362−23370.
(28) Liao, H.-C.; Tsao, C.-S.; Lin, T.-H.; Chuang, C.-M.; Chen, C.-Y.; Jeng, U.-S.; Su, C.-H.; Chen, Y.-F.; Su, W.-F. Quantitative Nanoorganized Structural Evolution for a High Efficiency Bulk Heterojunction Polymer Solar Cell. *J. Am. Chem. Soc.* **2011**, *133*, 13064−13073.
(29) Kaune, G.; Ruderer, M. A.; Metwalli, E.; Wang, W.; Couet, S.; Schlage, K.; Röhlsberger, R.; Roth, S. V; Müller-Buschbaum, P. In Situ GISAXS Study of Gold Film Growth on Conducting Polymer Films. *ACS Appl. Mater. Interfaces* **2009**, *1*, 353−360.
(30) Kaune, G.; Metwalli, E.; Meier, R.; Körstgens, V.; Schlage, K.; Couet, S.; Röhlsberger, R.; Roth, S. V; Müller-Buschbaum, P. Growth and Morphology of Sputtered Aluminum Thin Films on P3HT Surfaces. *ACS Appl. Mater. Interfaces* **2011**, *3*, 1055−1062.
(31) Schwartzkopf, M.; Buffet, A.; Körstgens, V.; Metwalli, E.; Schlage, K.; Benecke, G.; Perlich, J.; Rawolle, M.; Rothkirch, A.; Heidmann, B.; et al. From Atoms to Layers: In Situ Gold Cluster Growth Kinetics during Sputter Deposition. *Nanoscale* **2013**, *5*, 5053−5062.
(32) Metwalli, E.; Couet, S.; Schlage, K.; Röhlsberger, R.; Körstgens, V.; Ruderer, M.; Wang, W.; Kaune, G.; Roth, S. V; Müller-Buschbaum, P. In Situ GISAXS Investigation of Gold Sputtering onto a Polymer Template. *Langmuir* **2008**, *24*, 4265−4272.
(33) Döhrmann, R.; Botta, S.; Buffet, A.; Santoro, G.; Schlage, K.; Schwartzkopf, M.; Bommel, S.; Risch, J. F. H.; Mannweiler, R.; Brunner, S.; et al. A New Highly Automated Sputter Equipment for in Situ Investigation of Deposition Processes with Synchrotron Radiation. *Rev. Sci. Instrum.* **2013**, *84*, 043901−043908.
(34) Buffet, A.; Rothkirch, A.; Döhrmann, R.; Körstgens, V.; Abul Kashem, M. M.; Perlich, J.; Herzog, G.; Schwartzkopf, M.; Gehrke, R.; Müller-Buschbaum, P.; et al. P03, the Microfocus and Nanofocus X-ray

Scattering (Minaxs) Beamline of the PETRA III Storage Ring: The Microfocus Endstation. *J. Synch. Rad.* **2012**, *19*, 647−653.
(35) Metwalli, E.; Körstgens, V.; Schlage, K.; Meier, R.; Kaune, G.; Buffet, A.; Couet, S.; Roth, S. V; Röhlsberger, R.; Müller-Buschbaum, P. Cobalt Nanoparticles Growth on a Block Copolymer Thin Film: A Time-Resolved GISAXS Study. *Langmuir* **2013**, *29*, 6331−6340.
(36) Yoneda, Y. Anomalous Surface Reflection of X-rays. *Phys. Rev.* **1963**, *131*, 2010−2013.
(37) Malliaras, G. G.; Shen, Y.; Dunlap, D. H.; Murata, H.; Kafafi, Z. H. Nondispersive Electron Transport in Alq3. *Appl. Phys. Lett.* **2001**, *79*, 2582−2584.